European Journal of Medicinal Chemistry 83 (2014) 685–694

Contents lists available at ScienceDirect

European Journal of Medicinal Chemistry

journal homepage: http://www.elsevier.com/locate/ejmech

Original article

Synthesis, spectroscopic properties and photodynamic activity of porphyrin–fullerene C_{60} dyads with application in the photodynamic inactivation of *Staphylococcus aureus*

M. Belén Ballatore, Mariana B. Spesia, M. Elisa Milanesio, Edgardo N. Durantini*

Departamento de Química, Facultad de Ciencias Exactas Físico-Químicas y Naturales, Universidad Nacional de Río Cuarto, Agencia Postal Nro 3, X5804BYA Río Cuarto, Córdoba, Argentina

ARTICLE INFO

Article history:
Received 11 March 2014
Received in revised form
29 June 2014
Accepted 30 June 2014
Available online 1 July 2014

Keywords:
Porphyrin
Fullerene
Photosensitizer
Photodynamic inactivation
Dyads
Staphylococcus aureus

ABSTRACT

A covalently linked porphyrin–fullerene C_{60} dyad **5** was synthesized by 1,3-dipolar cycloaddition using 5-(4-formylphenyl)-10,15,20-tris[3-(*N*-ethylcarbazoyl)]porphyrin, *N*-methylglycine and fullerene C_{60}. Methylation of **5** was used to obtain a cationic dyad **6**. Spectroscopic properties were compared in toluene, *N*,*N*-dimethylformamide (DMF) and toluene/sodium bis(2-ethylhexyl)sulfosuccinate (AOT)/water reverse micelles. Absorption spectra of the dyads were essentially a superposition of the spectra of the porphyrin and fullerene reference compounds, indicating a very weak interaction between the chromophores in the ground state. The fluorescence emission of the porphyrin moiety in the dyads was strongly quenched by the attached fullerene C_{60} unit. The singlet molecular oxygen, $O_2(^1\Delta_g)$, productions (Φ_Δ) were strongly dependent on the solvent polarity. Similar Φ_Δ values were obtained for 5,10,15,20-tetrakis[3-(*N*-ethylcarbazoyl)]porphyrin (TCP) in both solvents. Also, dyad **5** showed a high $O_2(^1\Delta_g)$ generation in toluene. However, $O_2(^1\Delta_g)$ production mediated by **5** considerably diminished in the more polar solvent DMF. Also, a high photodynamic activity involving $O_2(^1\Delta_g)$ was found for both dyads in a simple biomimetic system formed by AOT reverse micelles. The photoinactivation ability of these dyads was investigated in *Staphylococcus aureus* cell suspensions. Photosensitized inactivation of *S. aureus* by dyad **6** exhibits a 4.5 log decrease of cell survival (99.997% cell inactivation), when the cultures are treated with 5 μM photosensitizer and irradiated with visible light (350–800 nm) for 30 min. Under these conditions, a lower photocytotoxic effect was found for **5** (3.2 log decrease). Furthermore, photoinactivation induced by **6** was higher than those obtained with the separate moieties of the dyad. Therefore, molecular structures formed by porphyrin–fullerene C_{60} dyads represent interesting photosensitizers to inactivate *S. aureus*.

1. Introduction

Staphylococcus aureus is a leading cause of human bacterial infections worldwide [1]. The severity of these infections varies widely from minor skin infections to fatal necrotizing pneumonia. Also, *S. aureus* has outstanding ability to acquire resistance to antibiotics [2]. This resistance is of great concern because antibiotics are absolutely crucial for treatment of many types of bacterial infections. Antibiotic-resistant *S. aureus* is endemic in hospitals worldwide, and causes substantial morbidity and mortality. Therefore, it is imperative to provide perspectives for the future prophylaxis or new treatments for *S. aureus* infections. In this sense, photodynamic inactivation (PDI) of microorganisms has been proposed as an alternative to controlling bacterial infections [3]. This approach combines a photosensitizer, visible light and oxygen to yield highly reactive oxygen species (ROS), which rapidly react with a variety of substrates producing damages in the biomolecules. These changes generate a loss of biological functionality leading to cell inactivation [4]. In PDI, two photoprocesses are mainly involved after activation of the photosensitizer [5]. In the type I pathway, the photosensitizer interacts with substrates to produce free radicals. These radicals can react with oxygen yielding a complex mixture of ROS. In the type II mechanism, singlet molecular oxygen, $O_2(^1\Delta_g)$, is produced by energy transfer from the photosensitizer. Thus, the prevailing mechanism can be influenced by the photosensitizer, the presence of substrates and the microenvironment where the agent is located [6].

* Corresponding author.
E-mail address: edurantini@exa.unrc.edu.ar (E.N. Durantini).

http://dx.doi.org/10.1016/j.ejmech.2014.06.077
0223-5234/

Generally, effective photosensitizers for PDI exhibit a high absorption coefficient in the visible region of the spectrum and a long lifetime of triplet excited state to produce efficiently ROS. Thus, several porphyrins with intrinsic positive charges meet these requirements and they have been successfully tested as photoinactivating agents against microorganisms [3,4]. Also, an interesting behavior was observed in fullerene C_{60} linked to an electron donor molecular structure, such as porphyrins [7]. These dyads present higher capacity to form photoinduced charge-separated state [8–10]. Therefore, the electron transfer process can compete with the $O_2(^1\Delta_g)$ production [11]. Previous studies revealed that fullerene C_{60} covalently attached to a porphyrin substituted by methoxy groups and its metal complex with Zn(II) were effective photosensitizers to kill Hep-2 human larynx carcinoma cell line [12,13]. Thus, depending on the microenvironment where the photosensitizer is localized, this compound could produce a biological photodamage through either a $O_2(^1\Delta_g)$-mediated photoreaction process or a free radical mechanism under low oxygen concentration. Hence, these dyads have offered a promising molecular architecture for photosensitizer agents that can produce cellular inactivation under anoxic conditions [12,13].

In the present study, a novel porphyrin–fullerene C_{60} dyad **5** was synthetized, which contain three carbazoyl groups attached to the tetrapyrrolic macrocycle at the *meso* positions. Many condensed heterocyclic compounds containing a carbazole nucleus have been reported to develop a broad range of potent biological activities [14]. Also, porphyrins connected to peripheral carbazole units represent efficient light-harvesting structures, where the carbazole groups can act as antenna at lower wavelengths [15,16]. The nitrogen atoms in the carbazole units were used to obtain dyad **6** bearing cationic groups on the periphery of the macrocycle. The formation of cationic amphiphilic photosensitizers has several interesting features that make these compounds attractive photosensitizers for a variety of biological systems [4,17]. The spectroscopic and photodynamic properties of these dyads were studied in homogeneous media of different polarities and in a simple biomimetic system formed by reverse micelles. The results obtained for these dyads were compared with those of porphyrin and fullerene reference compounds. Photodynamic action was then evaluated *in vitro* for inactivation of *S. aureus* cells.

2. Materials and methods

2.1. General

Proton nuclear magnetic resonance spectra were performed on a FT-NMR Bruker Avance DPX400 spectrometer at 400 MHz. Mass Spectra were recorded on a Bruker micrOTOF-QII (Bruker Daltonics, MA, USA) equipped with an atmospheric pressure photoionization (APPI) source. FT-IR spectra were recorded on a Nicolet Impact 400 (Madison, WI, USA). Absorption and fluorescence spectra were carried out in a Shimadzu UV-2401PC spectrometer (Shimadzu Corporation, Tokyo, Japan) and on a Spex FluoroMax spectrofluorometer (Horiba Jobin Yvon Inc, Edison, NJ, USA), respectively. The visible light source used to irradiate cell suspensions was a Novamat 130 AF (Braun Photo Technik, Nürnberg, Germany) slide projector containing a 150 W lamp. A 2.5 cm glass cuvette filled with water was used to remove the heat from the lamp. A wavelength range between 350 and 800 nm was selected by optical filters. The fluence rate was determined as 90 mW/cm^2 (Radiometer Laser Mate-Q, Coherent, Santa Clara, CA, USA).

All the chemicals from Aldrich (Milwaukee, WI, USA) were used without further purification. Sodium bis(2-ethylhexyl)sulfosuccinate (AOT) from Sigma (St. Louis, MO, USA) was dried under vacuum. Silica gel thin-layer chromatography (TLC) plates 250 microns from Analtech (Newark, DE, USA) were used. Solvents (GR grade) from Merck (Darmstadt, Germany) were distilled. Ultrapure water was obtained from a Labconco (Kansas, MO, USA) equipment model 90901-01.

2.2. Synthesis

5,10,15,20-Tetrakis(4-methoxyphenyl)porphyrin (TMP) was purchased from Aldrich. 4-(5,5-Dimethyl-1,3-dioxan-2-yl)benzaldehyde **2**, *N*-methyl-2-phenylfulleropyrrolidine (MPC_{60}), *N*,*N*-dimethyl-2-(4′-acetamidophenyl)fulleropyrrolidinium (DAC_{60}^{+}) and 5,10,15,20-tetrakis[3-(*N*-ethyl-*N*-methylcarbazoyl)]porphyrin (TCP^{4+}) were synthesized as previously described [18–21]. Synthesis procedures of porphyrin derivatives and dyads are shown in Schemes 1 and 2.

2.2.1. *meso*-(*N*-Ethyl-3-carbazoyl)dipyrromethane **1**

A solution of *N*-ethyl-3-carbazolecarboxaldehyde (1.01 g, 4.52 mmol), pyrrole (50.0 mL, 722.75 mmol) and TFA (65 μL, 0.85 mmol) was treated following the methodology reported before [15]. After work up, this approach yielded 1.36 g (89%) of dipyrromethane **1**.

2.2.2. 5-(4-(5,5-Dimethyl-1,3-dioxan-2-yl)phenyl)-10,15,20-tris[3-(*N*-ethylcarbazoyl)]porphyrin **3**

A solution of *N*-ethyl-3-carbazolecarboxaldehyde (289 mg, 1.29 mmol), benzaldehyde **2** (355 mg, 1.61 mmol) and dipyrromethane **1** (1.10 g, 3.24 mmol) in 365 mL of chloroform was purged with argon for 30 min. Then, trifluoroacetic acid (TFA, 500 μL, 6.50 mmol) was added. The solution was stirred for 30 min at room temperature and after that triethylamine (TEA, 1 mL, 7.20 mmol) was added. Then, 2,3-dichloro-5,6-dicyano-1,4-benzoquinone (DDQ, 2.50 g, 11.00 mmol) was added and the mixture was stirred for an additional 3 h at room temperature. The solvent was evaporated under reduced pressure. Flash column chromatography (silica gel, cyclohexane/chloroform (1:9) to chloroform gradient) yielded 251 mg (18%) of pure porphyrin **3** as second moving purple band. TLC (chloroform) analysis $R_f = 0.42$. ^{1}H NMR ($CDCl_3$, TMS) δ [ppm]: −2.48 (2H, pyrrole NH); 0.92 (s, 3H, $-CH_3$); 1.29 (s, 3H, $-CH_3$); 1.69 (t, 9H, $J = 7.1$ Hz, carbazole$-CH_3$); 3.85 (d, 2H, $-CH_2-$, $J = 10.8$ Hz); 3.97 (d, 2H, $-CH_2-$, $J = 10.8$ Hz); 4.63 (q, 6H, $J = 7.1$ Hz carbazole-CH_2); 5.75 (s, 1H, −CH−); 7.31 (m, 3H, Ar carbazole); 7.59 (m, 6H, Ar carbazole); 7.76 (d, 3H, Ar carbazole, $J = 8.2$ Hz); 7.93 (d, 2H, 5-Ar 3, 5-H, $J = 7.9$ Hz); 8.22 (d, 3H, Ar carbazole, $J = 8.0$ Hz); 8.31 (d, 2H, 5-Ar 2, 6-H, $J = 7.9$ Hz); 8.38 (d, 3H, Ar carbazole, $J = 8.2$ Hz); 8.88 (d, 2H, pyrrole, $J = 5.0$ Hz); 8.92 (m, 6H, pyrrole); 8.99 (s, 3H, Ar carbazole). ESI-MS [*m*/*z*] 1080.4965 $[M+H]^+$ (1079.4887 calculated for $C_{74}H_{61}N_7O_2$). Also, the condensation under these conditions produced 5,10,15,20-tetrakis[3-(*N*-ethylcarbazoyl)]porphyrin (TCP), which was obtained as the first moving purple band (84 mg, 12%). Spectroscopic data of TCP agree with those previously reported [15].

2.2.3. 5-(4-Formylphenyl)-10,15,20-tris[3-(*N*-ethylcarbazoyl)] porphyrin **4**

Porphyrin **3** (261 mg, 0.24 mmol) was hydrolyzed with 5 mL of TFA in 12 mL of a heterogeneous mixture of chloroform/water (1:1). The reaction was stirred at room temperature for 30 h. Then, the mixture was washed with water (10 mL each) for two times, the organic phase neutralized with TEA and washed with water (8 mL). Removal of the solvent under vacuum yielded 228 mg (95%) of the desired porphyrin **4**. TLC (chloroform/TEA 5%) analysis $R_f = 0.86$. ^{1}H NMR ($CDCl_3$, TMS) δ [ppm]: −2.50 (2H, pyrrole NH); 1.68 (t, 9H, $J = 7.1$ Hz, carbazole-CH_3); 4.63 (q, 6H, $J = 7.1$ Hz carbazole-CH_2); 7.29 (m, 3H, Ar carbazole); 7.58 (m, 6H, Ar carbazole); 7.75 (d, 3H, Ar

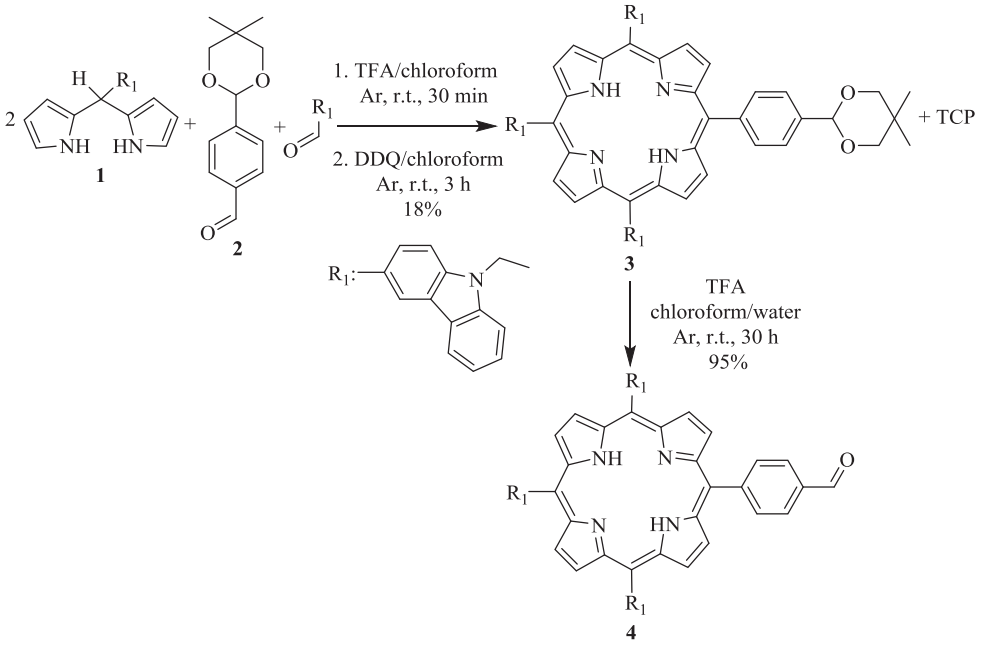

Scheme 1. Synthesis of aldehyde porphyrin **4**.

carbazole, $J = 8.5$ Hz); 8.28 (d, 2H, 5-Ar 3, 5-H, $J = 8.0$ Hz); 8.19 (d, 3H, Ar carbazole, $J = 8.0$ Hz); 8.44 (d, 2H, 5-Ar 2, 6-H, $J = 8.0$ Hz); 8.34 (d, 3H, Ar carbazole, $J = 8.4$ Hz); 8.77 (d, 2H, pyrrole, $J = 5.0$ Hz); 8.87–8.98 (m, 9H, pyrrole and Ar carbazole), 10.37 (s, 1H, Ar–CHO). ESI-MS [*m*/*z*] 994.4233 $[M+H]^+$ (993.4155 calculated for $C_{69}H_{51}N_7O$).

2.2.4. Dyad **5**

A solution of fullerene C_{60} (158 mg, 0.22 mmol), porphyrin **4** (212 mg, 0.21 mmol) and *N*-methylglycine (37 mg, 0.42 mmol) in 150 mL of dry toluene was stirred at reflux in atmosphere of argon for 18 h. Then, the solvent was removed under vacuum. Flash column chromatography (silica gel) using toluene as eluent afforded 230 mg (62%) of pure **5**. TLC (toluene) $R_f = 0.53$. ^{1}H NMR ($CDCl_3$, TMS) δ [ppm]: −2.53 (2H, pyrrole NH); 1.67 (t, 9H, carbazole-CH_3, $J = 6.9$ Hz); 2.91 (s, 3H, N-CH_3 pyrrolidine ring); 4.22 (d, 1H, pyrrolidine ring, 9.0 Hz), 4.96–5.04 (m, 2H, pyrrolidine ring 9.4 Hz); 4.62 (q, 6H, carbazole-CH_2, $J = 6.9$ Hz); 7.30 (m, 3H, Ar carbazole); 7.58 (m, 6H, Ar carbazole); 7.74 (d, 3H, Ar carbazole, $J = 8.2$ Hz); 7.82 (d, 2H, 5-Ar 3,5-H, $J = 7.9$ Hz); 8.18 (d, 3H, Ar carbazole, $J = 8.1$ Hz); 8.27 (d, 2H, 5-Ar 2,6-H, $J = 7.9$ Hz); 8.35 (d, 3H, Ar carbazole, $J = 8.2$ Hz); 8.84–8.98 (m, 11H, pyrrole and Ar carbazole). ESI-MS [*m*/*z*] 1741.4706 $[M+H]^+$ (1740.4628 calculated for $C_{131}H_{56}N_8$).

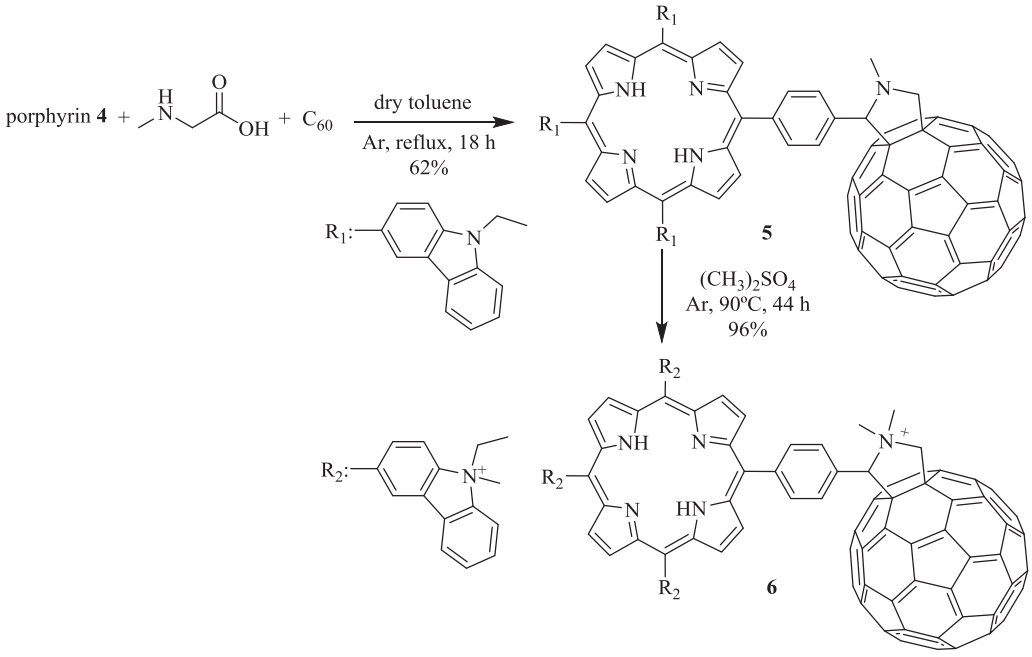

Scheme 2. Synthesis of porphyrin-C_{60} dyads **5** and **6**.

2.2.5. Dyad **6**

A mixture of **5** (10 mg, 6×10^{-3} mmol) and dimethyl sulfate (2 mL, 21.10 mmol) was stirred for 44 h at 90 °C. The mixture was placed in Eppendorf pipettes and ethyl ether was added. The methylated dyad was precipitated. It was washed with 5% aqueous Na_2CO_3 and then with water to obtain 96% of **6**. FT-IR (KBr) ν [cm^{-1}]: 2976, 2937, 2874, 1595, 1470, 1400, 1230, 1166, 1037, 850, 806, 525. ESI-MS [m/z] 1801.5645 $[M+H]^+$ (1800.5567 calculated for $C_{135}H_{68}N_8$).

2.3. Spectroscopic studies

Absorption and fluorescence spectra were performed in a quartz cell of 1 cm path length using DMF, toluene and toluene/AOT (0.1 M)/water ($W_0 = 10$) media at 25.0 ± 0.5 °C. Absorbances (<0.05) were matched at the excitation wavelength (550 nm) and the areas of the emission spectra were integrated in the range 600–800 nm. The energy of the singlet state (E_s) was calculated from the intersection of the normalized absorption and fluorescence curves. The fluorescence quantum yield (Φ_F) of the photosensitizers was calculated by comparison of the area below the corrected emission spectrum in each solvent with that of TMP as a reference. For this purpose, the values of Φ_F for TMP in DMF ($\Phi_F^{DMF} = 0.14$) and in toluene ($\Phi_F^{toluene} = 0.12$) were calculated by comparison with the fluorescence spectrum in tetrahydrofuran using $\Phi_F = 0.14$ for TMP and taking into account the refractive index of the solvents [22].

2.4. Steady state photolysis

Solutions of 9,10-dimethylanthracene (DMA, 35 μM) and photosensitizer in DMF and toluene were irradiated in 1 cm path length quartz cell (2 mL) with monochromatic light at $\lambda_{irr} = 428$ nm (photosensitizer absorbance 0.1), from a Cole–Parmer illuminator 41720-series (Cole–Parmer, Vernon Hills, IL, USA) with a 150 W halogen lamp through a high intensity grating monochromator (Photon Technology Instrument, Birmingham, NJ, USA). The light fluence rate was determined as 0.36 mW/cm^2. The kinetics of DMA photooxidation were studied following the decrease of the absorbance (A) at $\lambda_{max} = 379$ nm. The observed rate constants (k_{obs}) were obtained by a linear least-squares fit of the semilogarithmic plot of Ln A_0/A *vs.* time. Quantum yields of $O_2(^1\Delta_g)$ production (Φ_Δ) were calculated comparing the k_{obs} for the corresponding photosensitizer with that for TMP, which was used as a reference ($\Phi_\Delta^{DMF} = 0.65$ and $\Phi_\Delta^{toluene} = 0.67$) [22]. Measurements of the sample and reference under the same conditions afforded Φ_Δ for photosensitizers by direct comparison of the slopes in the linear region of the plots.

2.5. Studies in AOT reverse micelles

A stock solution of 0.1 M AOT was prepared by weighing and dilution in toluene. The amount of water present in the system was expressed as the molar ratio between water and the AOT present in the reverse micelle ($W_0 = [H_2O]/[AOT]$). In all experiments, $W_0 = 10$ was used and the mixtures were sonicated for about 10 s to obtain perfectly clear micellar system [23]. A calibrated microsyringe was used for the addition of water to the corresponding solution.

The two pseudophase model was used to evaluate the distribution of photosensitizer between the AOT reverse micelles and the toluene [24]. The distribution constant, $K_{AOT} = [\text{photosensitizer}_b]/[\text{photosensitizer}_f][AOT]$ (where [AOT] is the surfactant concentration and the terms $[\text{photosensitizer}_b]$ and $[\text{photosensitizer}_f]$ refer to the concentration of bound and free photosensitizer, respectively) were determined from the emission spectral changes at the $Q_x(0-0)$ band upon varying the AOT concentration. Values of K_{AOT} were calculated by nonlinear fitting of the experimental data using Equation (1) [24]:

$$I^\lambda = \frac{[\text{photosensitizer}]_0\left(\Phi_{Ff} + \Phi_{Fb}K_{AOT}[AOT]\right)}{(1 + K_{AOT}[AOT])} \quad (1)$$

where I^λ is the emission intensity at different [AOT], $[\text{photosensitizer}]_0$ is the initial concentration of the photosensitizer, Φ_{Ff} and Φ_{Fb} are the fluorescence quantum yields for the photosensitizer in toluene and bound to the micelles, respectively. This equation applies at a fixed value of W_0 and when $[\text{photosensitizer}]_0 << [AOT]$.

Photosensitized decomposition of DMA was performed in reverse micelles as explained above in DMF. The values of Φ_Δ were calculated using TCP ($\Phi_\Delta^{toluene} = 0.42$) as reference because this porphyrin is mainly dissolved in the external solvent.

2.6. Bacterial strain and preparation of cultures

The microorganism used in this study was the reference strain *S. aureus* ATCC 25923. This bacterium was grown on a rotator shaker (100 rpm) at 37 °C in tryptic soy (TS, Britania, Buenos Aires, Argentina) broth overnight. The *Escherichia coli* strain (EC7) was previously characterized and identified [20]. *E. coli* was grown aerobically at 37 °C in TS broth overnight. Aliquots (~60 μL) of this culture was aseptically transferred to 4 mL of fresh medium and incubated with agitation at 37 °C to middle of the logarithmic phase (absorbance ~0.3 at 660 nm). Cells were centrifuged (3000 rpm for 15 min) and re-suspended in equal amount of 10 mM phosphate-buffered saline (PBS, pH = 7.0) solution. Then the cells were diluted 1/1000 in PBS, corresponding to ~10^6 colony forming units (CFU)/mL. In all the experiments, 2 mL of the cell suspensions in Pyrex brand culture tubes (13 × 100 mm) were used. Cellular suspensions were serially diluted with PBS and each solution was quantified by using the spread plate technique in triplicate. Viable bacteria were monitored and the number of CFU was determined on TS agar plates after ~24 h incubation at 37 °C.

2.7. Photosensitized inactivation of bacteria cells

Cell suspensions of *S. aureus* or *E. coli* (2 mL, ~10^6 CFU/mL) in PBS were treated with the corresponding photosensitizer at different concentrations (1 and 5 μM). The photosensitizer was added from a stock solution (~0.5 mM) in DMF. The cultures were incubated with agitation (100 rpm) in the dark at 37 °C for 30 min. Then the cell suspensions in Pyrex culture tubes (13 × 100 mm) were exposed for different time intervals (5, 15 and 30 min for *S. aureus* and 30 min for *E. coli*) to visible light using the irradiation system as described above. The solvent DMF of the photosensitizer was not toxic for bacteria. Serial dilutions of irradiated cell suspensions and controls were performed with PBS and each sample was plated in triplicate on TS agar. The number of colonies formed after ~24 h incubation at 37 °C was counted [20].

2.8. Controls and statistical analysis

Control experiments were performed in presence and absence of photosensitizer in the dark and in the absence of photosensitizer with cells irradiated. The amount of DMF used in each experiment was not toxic to *S. aureus* cells. Three values were obtained per each condition and each experiment was repeated separately three times. The unpaired t-test was used to establish the significance of differences between groups. Differences were considered statistically significant with a confidence level of 95% ($p < 0.05$). Data were represented as the mean ± standard deviation of each group.

3. Results and discussion

3.1. Synthesis of porphyrin-C_{60} dyads

The synthetic procedures to obtain porphyrins are summarized in Scheme 1. Porphyrins with AB_3-symmetry can be conveniently synthesized from a binary mixture of aldehydes and an appropriate dipyrromethane catalyzed by acid [25,26]. The application of this approach to the synthesis of porphyrin **3** required the previous formation of dipyrromethane **1**. Thus, compound **1** was obtained from the condensation of *N*-ethyl-3-carbazolecarboxaldehyde with a large excess of pyrrole (1:47 aldehyde/pyrrole mol ratio), catalyzed by TFA at room temperature. Flash chromatography on silica gel yield 89% of the product **1**, using cyclohexane/ethyl acetate/triethylamine (80:20:1) as eluent. On the other hand, one aldehyde function of the terephthaldicarboxaldehyde was protected to avoid multiple products in the MacDonald-type 2 + 2 condensation to form porphyrins [18]. Thus, the reaction of terephthaldicarboxaldehyde with 2,2-dimethylpropane-1,3-diol in the presence of a catalytic amount of *p*-toluensulfonic acid in refluxing toluene gave the protected 4-(4,4-dimethyl-2,6-dioxan-1-yl)benzaldehyde **2** in 70% yield. Acid-catalyzed condensation of dipyrromethane **1** with a binary mixture of *N*-ethyl-3-carbazolecarboxaldehyde and monoprotected benzaldehyde **2** was used to obtain porphyrin **3** (Scheme 1). The reaction was performed using a (0.8:1.0:2.0) molar relationship of *N*-ethyl-3-carbazolecarboxaldehyde, benzaldehyde **2** and dipyrromethane **1**, respectively. First, the mixture was reacted using catalytic amount of TFA and chloroform as solvent, at room temperature. The subsequent oxidative treatment with DDQ affords a mixture of porphyrins. The products were separated by flash column chromatography (silica gel) using gradient elution. First a mixture of cyclohexane/chloroform 90% was used and then chloroform. Under these conditions, the first band corresponding to TCP and the desired porphyrin **3** obtained in 18% yield as the second purple band. The hydrolysis of porphyrin **3** in the presence of an excess of TFA in chloroform/water (1:1) produces porphyrin **4** in 95% yield after stirring for 30 h at room temperature.

Finally, porphyrin-linked fullerene C_{60} dyad **5** was obtained by 1,3-dipolar cycloaddition in dry toluene using porphyrin **4**, *N*-methylglycine and fullerene C_{60}, (1.0:1.9:1.0) molar relationship, respectively (Scheme 2). The mixture was stirred for 18 h at reflux in an argon atmosphere. This reaction mixture produces dyad **5**, which was purified by flash chromatography (silica gel) with 62% yield. Similar approaches were previously used to obtain several porphyrin–fullerene C_{60} derivatives, which can produce photoinduced electron transfer [8,9]. The structure of dyad **5** was the precursor of a cationic dyad **6** by methylation. Thus, cationic dyad **6** was obtained by treating the dyad **5** with dimethyl sulphate for 44 h at 90 °C (Scheme 2). The exhaustive methylation produces dyad **6** in high yields (96%).

3.2. Absorption and fluorescence spectroscopic properties

The absorption spectra of the dyads and their monomer models for porphyrin and C_{60} moieties (Scheme 3) in different media are shown in Fig. 1. The absorption of the dyads in the UV region is higher than that of TCP due to the presence of the C_{60} moiety, whereas in the visible region the spectra of the dyads are quite similar to porphyrin. The fullerene C_{60} unit has moderately strong $\pi-\pi^*$ absorption bands in the UV region with maxima at 330 nm and in the visible region a broader range of absorption up to almost 750 nm, with a weak absorption broader band at 714 nm. These dyads showed the typical Soret band at ~430 nm and the four *Q*-bands between 515 and 650 nm, characteristic of *meso*-tetraphenylporphyrin derivatives [27]. The spectroscopic properties of the photosensitizers are summarized in Table 1. Sharp absorption Soret bands were obtained for both dyads **5** and **6**, indicating that the photosensitizers are mainly non-aggregated in DMF (Fig. 1). The Q band of the free base porphyrin moiety consists of four components: $Q_x(0,0)$, $Q_x(1,0)$, $Q_y(0,0)$ and $Q_y(1,0)$, which are associated with D_{2h} symmetry [28,29]. The maximum of the Soret band of carbazoyl porphyrin derivative shows an 12 nm bathochromic shift respect to TPP due to the *auxochromic effect* of the four carbazoyl groups [30]. As can be observed, the spectra of the dyads are essentially a linear combination of the spectra of the corresponding moieties, with only minor differences in wavelength maxima and band shapes. Thus the absorption spectra are consistent with only a weak interaction between the moieties in the ground state and both chromophores retain their individual identities. In general, not strong electronic interactions among the chromophores were found in porphyrin–fullerene C_{60} [9,31].

The spectra were also recorded in toluene and toluene/AOT (0.1)/water ($W_0 = 10$) reverse micelles. The spectrum of dyad **5** in toluene was very similar to that in DMF, indicating no aggregation (Fig. 1, inset). A small bathochromically effect of 2 nm in the maximum of the Soret band was produced in toluene with respect to DMF. Moreover, the shape of absorption bands of dyad **5** was quite similar in toluene and AOT system. On the other hand, charged dyad **6** showed two new bands in toluene, a more intense peak at 357 nm and a shoulder at 467 nm, possibly due to some partial aggregation in this less polar solvent. However, in toluene/AOT reverse micelles this band disappears and the absorption spectrum for charged dyad **6** resembled that obtained in DMF.

The steady-state fluorescence emission spectra of these dyads were compared with those of model porphyrins in DMF, exciting the samples at 550 nm (Fig. 2). The two bands around 665 and 730 nm are characteristic for similar *meso*-substituted porphyrin [16]. These bands have been assigned to $Q_x(0-0)$ and $Q_x(0-1)$ transitions [29]. This is a typical behavior for porphyrins with D_{2h} symmetry, like the free bases, and indicates that the porphyrin vibronic structure remains practically unchanged upon excitation [28]. From the intersection of the absorption and fluorescence

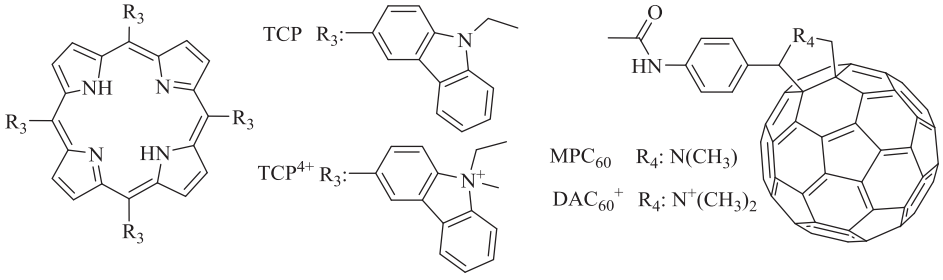

Scheme 3. Molecular structures of DAC_{60}^{+} and TCP^{4+}.

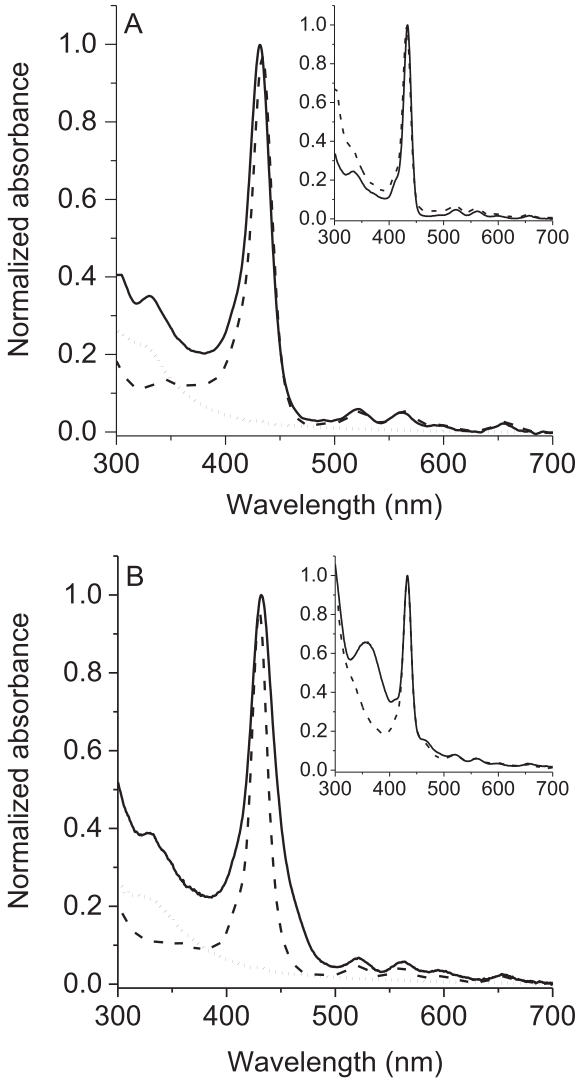

Fig. 1. Absorption spectra of (A) dyad **5** (solid line), TCP (dashed line) and MPC_{60} (dotted line) and (B) dyad **6** (solid line), TCP^{4+} (dashed line) and DAC_{60}^{+} (dotted line) in DMF. Inset: (A) **5** and (B) **6** in toluene (solid line) and toluene/AOT (0.1 M)/water ($W_0 = 10$) (dashed line).

spectra of the $Q_x(0–0)$ band, Stokes shifts of ~10 nm were calculated for the dyads. Small Stokes shifts indicated that in these molecules the spectroscopic energies are similar to the relaxed energies of the lowest singlet excited state S_1, according to the rigid planar structure of the tetrapyrrolic macrocycle. That suggests that only a minor geometric relaxation occurs in the first excited state. Similar spectra were also observed in toluene (see Fig. 4 inset, at [AOT] = 0). Fluorescence quantum yields (Φ_F) of these photosensitizers were calculated in DMF and toluene by comparison with TMP as a reference in the S_1 state (Table 1). The values of Φ_F for TCP and TCP^{4+} agree with values previously reported by similar porphyrin derivatives [21,32]. In contrast, both dyads show only very weak emission from the porphyrin moiety, indicating strong quenching of the porphyrin excited singlet state by the attached fullerene moiety. The quenching efficiencies were estimated to be $\eta_q \geq 0.96$ in DMF. These values are analogous to those previously reported for porphyrin derivatives attached to fullerene structure [7,31]. In these cases, the energy transfer from the locally excited porphyrin singlet state to the C_{60} moiety is an exothermic process. The energy levels of the singlet excited stated (E_s) were calculated taking into account the porphyrin energy of the 0–0 electronic transitions (Table 1). The free energy change for the initial charge separation giving $TCP^{\cdot+}$-$C_{60}^{\cdot-}$ was calculated from the radical ion pair and singlet state energies using the simplified Rehm-Weller equation $\Delta G_{CS} = e[E_0(P^{\cdot+}/P) - E_0(C_{60}/C_{60}^{\cdot-})] - E_S$, where $E_0(P^{\cdot+}/P)$ is the first oxidation potential of the donor (0.67 V DCE, SCE [16]), $E_0(C_{60}/C_{60}^{\cdot-})$ is the first reduction potential of the acceptor (−0.59 V DCE, SCE [19]), E_S is the singlet state energy of porphyrin (1.88 eV) [33,34]. For the initial charge separation from $^1TCP^*$ to C_{60}, a value of −0.62 eV for the driving force was obtained.

Table 1
Spectroscopic properties of photosensitizers in different media.

Photosensitizer	TCP	**5**	**6**
λ_{max}^{Soret} (nm)[a]	434	431	432
ε^{Soret} (M^{-1} cm^{-1})[a]	2.81×10^5	2.52×10^5	2.49×10^5
λ_{max}^{Em} (nm)[a]	667	667	664
E_s (eV)[a]	1.88	1.88	1.88
Φ_F^{DMF}	0.12 ± 0.02	(4.2 ± 0.3) × 10^{-3}	(4.9 ± 0.3) × 10^{-3}
$\Phi_F^{toluene}$	0.15 ± 0.02	(5.1 ± 0.4) × 10^{-3}	(3.5 ± 0.2) × 10^{-3}

[a] DMF.

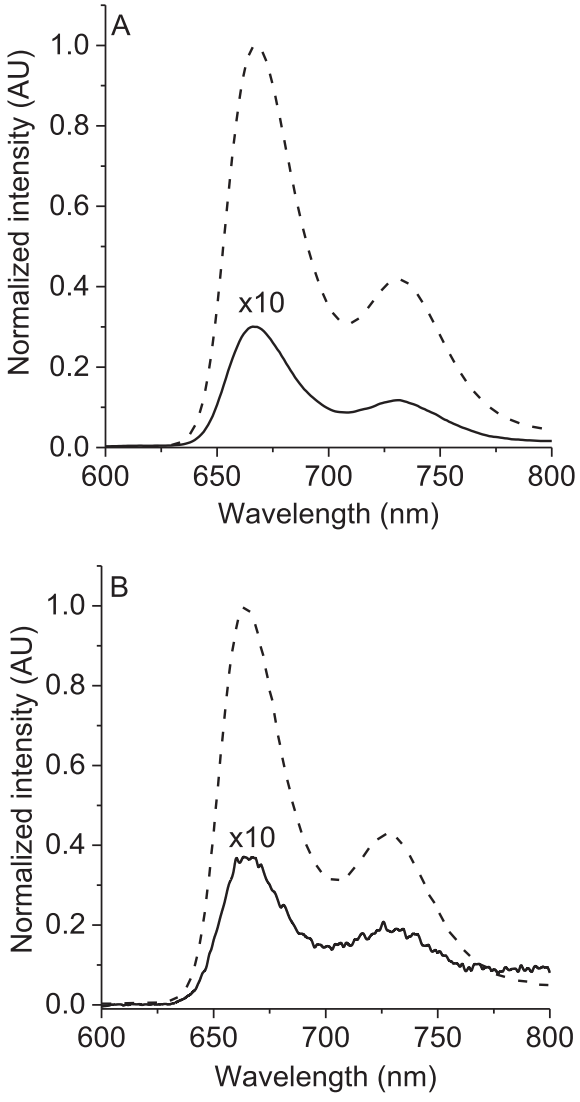

Fig. 2. Fluorescence emission spectra of (A) **5** (solid line) and TCP (dashed line) and (B) **6** (solid line) and TCP^{4+} (dashed line) in DMF (λ_{exc} = 550 nm).

3.3. Photosensitized decomposition of DMA

Photooxidation of DMA induced by these photosensitizers was compared in toluene and DMF under aerobic conditions. The samples were irradiated at 428 nm, where the absorption is mainly due to the presence of the tetrapyrrolic macrocycle. Therefore, the photophysical processes in the dyads **5** and **6** were initiated from the porphyrin unit. Fig. 3 shows characteristic semilogarithmic plots describing the progress of the reaction for DMA. The values of the observed rate constant (k_{obs}^{DMA}) were calculated from first-order kinetic plots of the DMA absorption at 379 nm with time (Table 2). In toluene, dyad **5** efficiently induced the decomposition of DMA, while non-reaction was detected using **6** as photosensitizer. This cationic dyad is not completely dissolved as monomers in toluene, as shown by absorption spectroscopy (Fig. 1(B) inset), and this partial aggregation inhibited the photodynamic activity. In DMF, the photooxidation rates of DMA mediated by both dyads considerably decrease in comparison with that of TCP. Therefore, a competitive process must be involved in this more polar solvent.

The kinetic data of DMA decomposition were used to estimate the quantum yield of $O_2(^1\Delta_g)$ production (Φ_Δ) because this substrate quenches $O_2(^1\Delta_g)$ by chemical reaction [35]. The values of Φ_Δ were calculated by comparing the slope for the photosensitizer with that for the reference (TMP) from the plots shown in Fig. 3. Comparable values of Φ_Δ were obtained for TCP in both solvents (Table 2), which are quite reasonable values for free base porphyrins dissolved as monomers [36]. A similar Φ_Δ value was previously reported for TCP in DMF [21]. On the other hand, in DMF the $O_2(^1\Delta_g)$ production significantly diminishes for the dyads with respect to that of TCP. In the case of **5**, the Φ_Δ value can be compared in both solvents and it was about 56 times lower in DMF than in toluene. Also, the production of Φ_Δ by **5** was 41 times lower than that of TCP in DMF. Moreover, a low value of Φ_Δ was found for **6** in the more polar medium. This behavior can be attributed to the formation of the charge-separated state, which is favored in a more polar solvent [9,11,12]. Thus, the Φ_Δ in both dyads was strongly dependent on the polarity of the microenvironment where the dyads are localized.

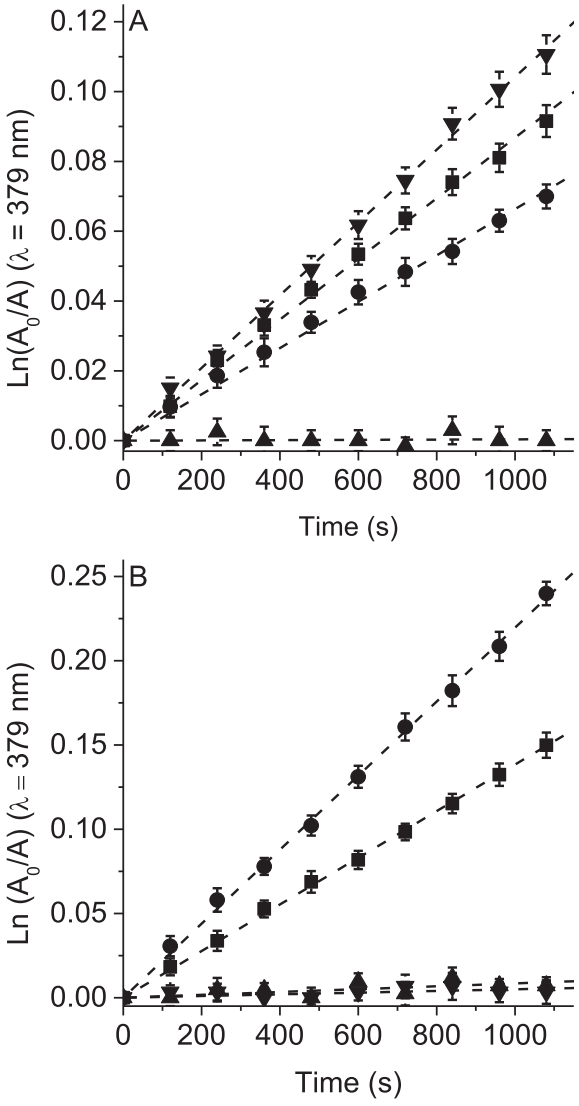

Fig. 3. First-order plots for the photooxidation of DMA (35 μM) photosensitized by **5** (▼), **6** (▲) TCP (■) and TMP (●) in (A) toluene and (B) DMF; λ_{irr} = 428 nm. Values represent mean ± standard deviation of three separate experiments.

Table 2
Kinetic parameters for the photooxidation reaction of DMA (k_{obs}) and singlet molecular oxygen quantum yield (Φ_Δ) in different media.

Photosensitizer	TCP	**5**	**6**
$k_{obs}^{toluene}$ (s^{-1})	$(0.66 \pm 0.01) \times 10^{-4}$	$(0.87 \pm 0.01) \times 10^{-4}$	NR[a]
$\Phi_\Delta^{toluene}$	0.42 ± 0.02[b]	0.56 ± 0.02	–
k_{obs}^{DMF} (s^{-1})	$(1.38 \pm 0.01) \times 10^{-4}$	$(5.0 \pm 0.9) \times 10^{-6}$	$(8.0 \pm 0.9) \times 10^{-6}$
Φ_Δ^{DMF}	0.41 ± 0.02[c]	0.010 ± 0.002	0.020 ± 0.003
k_{obs}^{AOT} (s^{-1})	$(3.6 \pm 0.1) \times 10^{-5}$	$(4.3 \pm 0.1) \times 10^{-5}$	$(3.9 \pm 0.1) \times 10^{-5}$
Φ_Δ^{AOT}	0.42 ± 0.02[d]	0.50 ± 0.02	0.46 ± 0.02

[a] Undetectable reaction.
[b] Using TMP as a reference $k_{obs}^{toluene} = (1.04 \pm 0.01) \times 10^{-4}$ s^{-1}.
[c] Using TMP as a reference $k_{obs}^{DMF} = (2.20 \pm 0.02) \times 10^{-4}$.
[d] Using TCP as a reference in toluene.

3.4. Solubilization and photodynamic activity of dyads in AOT reverse micelles

The solubilization and distribution of these dyads were spectroscopically analyzed in toluene/AOT (0.1 M)/water (W_0 = 10) reverse micelles. Many biological processes occur at the surface of membranes or within their hydrophobic moiety. Microheterogeneous media containing AOT have been used as a very simplified model of the membranes [37,38]. The presence of polar headgroups and hydrophobic chains in micellar structures allows studying the affinity of a great variety of photosensitizer to membrane. Therefore, in a micellar system a solute can be located in a variety of microenvironments, namely the organic surrounded solvent, the water pool or at the micellar interface [24]. When the fluorescence emission spectra of photosensitizers were studied at various AOT concentrations, an increase in the intensity of the emission bands was observed for both dyads as the surfactant concentration increased. Representative results for **5** and **6** are shown in Fig. 4 inset. This effect was attributed to the interaction between the dyad and the AOT micelles. Plotting the fluorescence emission intensity *vs.* AOT concentration, the value of the distribution constant (K_{AOT}) was calculated by fitting Equation (1) (Fig. 4). Values of K_{AOT} = 63 ± 10 M^{-1} for **5** and K_{AOT} = 432 ± 36 M^{-1} for **6** indicated that these photosensitizers were associated with the micelles. The presence of intrinsic positive charges in the macrocycle of **6** produced a higher interaction with AOT reverse micelles in comparison with its homolog containing amino groups. On the other hand, spectroscopic changes were not observed for TCP varying the AOT concentration (results not shown) indicating that this porphyrin remains solubilized in the toluene.

Photooxidation of DMA induced by these dyads was performed in toluene/AOT (0.1 M)/water (W_0 = 10) under aerobic conditions.

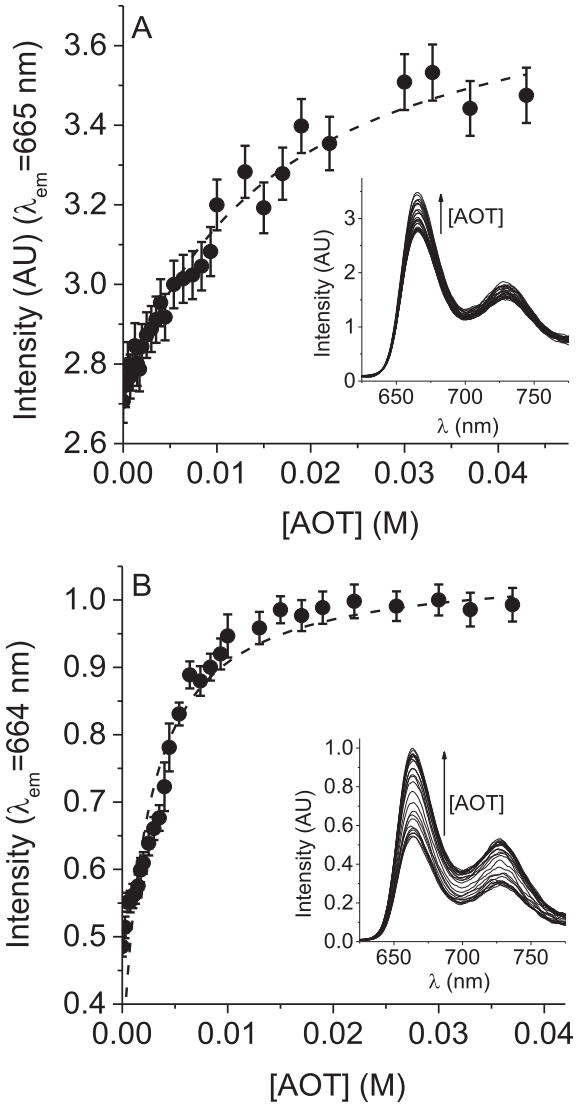

Fig. 4. Variation of fluorescence emission intensity as a function of [AOT] in toluene/AOT/water (W_0 = 10) reverse micelles of (A) **5** (λ_{max} = 665 nm) and (B) **6** (λ_{max} = 664 nm), λ_{exc} = 432 nm. Dashed line: no linear regression fit by Equation (1). Inset: fluorescence emission spectra of (A) **5** and (B) **6** at different AOT concentrations (0.25–37.0 mM). Values represent mean ± standard deviation of three separate experiments.

Because DMA is a non-polar compound, it is assumed that this substrate was mainly solubilized in the organic pseudophase (toluene) of the micellar system [39]. In this biomimetic microenvironment, the substrate reacted with the $O_2(^1\Delta_g)$ produced by photosensitization by the triplet excited states of the dyads. From the plots in Fig. 5, the values of the k_{obs}^{DMA} were calculated for DMA reaction in the micellar system. As can be observed in Table 2, the decomposition rates of DMA photosensitized by **5** and TCP showed the same tendency observed in toluene. However, the reaction rates of DMA sensitized by TCP and **5** in the AOT micellar system were slower than those found in toluene (Table 2) by a factor of ~2. Similar behavior was previously observed in AOT reverse micelles using porphyrins as photosensitizers [30]. In the AOT micellar system, $O_2(^1\Delta_g)$ is partitioned between the internal and external pseudophases [39]. Therefore, we propose that the photooxidation rate of DMA is diminished in the organic pseudophase.

In contrast to those observed in toluene or DMF, **6** efficiently photosensitized the decomposition of DMA in the AOT micellar system (Table 2). Two effects can be involved in this different behavior. First, the cationic dyad was partially aggregated in toluene homogenous media. Nevertheless, the AOT reverse micelles helped disaggregate the **6** dyad, which results in an increase in the photodynamic activity. Second, even though this dyad interacts strongly with the AOT micelles, due to the high lipophilic character of the fullerene sphere, it is expected that **6** will be located at the micellar interface with the moiety of the C_{60} placed at the non-polar solvent. Localization of C_{60} in the toluene pseudophase decrease the formation of the charge-separation state, favoring the photosensitization of $O_2(^1\Delta_g)$ from the fullerene triplet state. Moreover, considering that TCP is mainly solubilized in the toluene pseudophase, it was used as a reference to estimate the Φ_Δ values of the dyads in the AOT reverse micelles. As can be observed in Table 2, dyads **5** and **6** both acted as efficient photosensitizers to generate $O_2(^1\Delta_g)$ in this microheterogeneous medium.

3.5. Photosensitized inactivation of S. aureus

The photodynamic action induced by **5** and **6** to inactivate *S. aureus* bacterium was compared *in vitro*. This bacterium was selected due to its permeable outer membrane that allows for the diffusion of agents, as a defense mechanism [1]. Thus, suspensions of *S. aureus* cells in PBS were treated with 1 and 5 μM photosensitizer for 30 min in the dark at 37 °C and the cultures were then irradiated with visible light. Fig. 6 shows the survival of bacterial cells after different irradiation times (5, 15 and 30 min). Control experiments demonstrate that the viability of *S. aureus* was unaffected by illumination alone or by dark incubation with these photosensitizers for 30 min. Therefore, the cell inactivation observed after irradiation of the cultures treated with the photosensitizers was mediated by the photosensitization activity of the agents. Because of the multichromophoric nature of the dyads **5** and **6**, it can be expected that the corresponding results could change depending on which chromophore was excited. In the bacteria photoinactivation studies, the cultures were irradiated with visible light. Thus, both chromophores can be excited and a contribution of C_{60} moiety can be also involved in the inactivation of the microorganisms.

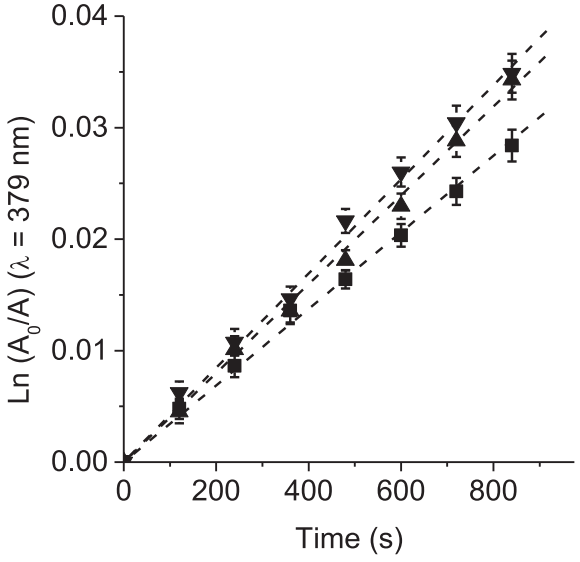

Fig. 5. First-order plots for the photooxidation of DMA (35 μM) photosensitized by **5** (▼), **6** (▲) and TCP (■) in toluene/AOT (0.1 M)/water (W_0 = 10); λ_{irr} = 428 nm. Values represent mean ± standard deviation of three separate experiments.

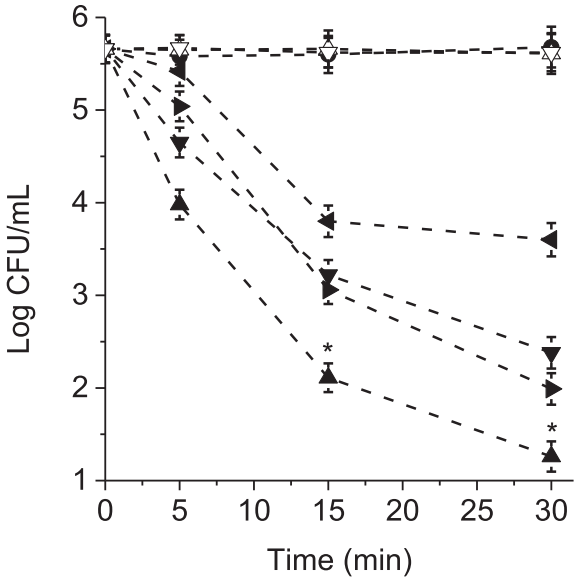

Fig. 6. Survival curves of *S. aureus* cells (~10^6 CFU/mL) incubated with 1 μM **5** (◄), 5 μM **5** (▼), 1 μM **6** (►) and 5 μM **6** (▲) for 30 min at 37 °C in dark and exposed to visible light for different irradiation times. Control cultures: cells treated 5 μM **5** (▽) and **6** (△) in dark; cells untreated with the photosensitizer and irradiated (●). Values represent mean ± standard deviation of three separate experiments (*$p < 0.05$, compared with **5**).

The photoinactivation of *S. aureus* cells was dependent on dyad concentrations and irradiation times. As seen in Fig. 6, the *S. aureus* cells are rapidly photoinactivated when the cultures treated with dyads were exposed to visible light. Bacterial suspension treated with 1 μM **5** and irradiated for 30 min produced a 2 log decrease in the viability, while 5 μM of this dyad exhibited a photosensitizing activity of 3.2 log units. A slightly higher photoinactivation was found using 1 μM **6** than 5 μM **5**. In particular, the cationic dyad **6** exhibited a photosensitizing activity causing a 4.5 log decrease of cell survival, when the cultures are treated with 5 μM dyad and irradiated for 30 min with visible light. These results represent a value greater than 99.997% of cellular inactivation. Therefore, at both concentrations, PDI mediated by **6** was significantly ($p < 0.05$) more effective than by **5**.

Moreover, the photoinactivation of *S. aureus* cells in PBS induced by **6** was compared with those of cationic DAC_{60}^{+} and TCP^{4+} (Scheme 3) using 1 μM photosensitizer at different irradiation times. As can be observed in Fig. 7, after 30 min of irradiation with visible light the fullerene derivative DAC_{60}^{+} inactivated only 1 log, while the tetracationic porphyrin TCP^{4+} achieved 2 log. Under these conditions, a decrease of 3.6 log was found in presence of **6**. PDI produced by dyad **6** was also evaluated in comparison with those reference compounds at 5 μM. This concentration of photosensitizers was not toxic in dark. The results indicated that DAC_{60}^{+} and TCP^{4+} induced a 1.7 log and 2.5 log decrease in survivals, respectively, while no colony formation was found with dyad **6**. At both concentrations, the results of the dyad **6** significantly differ ($p < 0.05$) from those of the reference compounds. Therefore, photoinactivation of *S. aureus* induced by **6** was higher than its individual cationic moieties, represented by DAC_{60}^{+} and TCP^{4+}.

Direct comparisons with other photosensitizers already described are difficult mainly due to different cell densities and irradiation systems used. For instance, 5,10,15,20-tetrakis(4-*N*,*N*,*N*-trimethylammoniumphenyl)porphyrin ($TMAP^{4+}$) and 5,10,15,20-tetrakis(4-*N*-methylpyridyl) porphyrin ($TMPyP^{4+}$) are known to act as photosensitizers in eradication of microorganisms [40,41]. In previous studies, *S. aureus* showed a dose-dependent photoinactivation when treated with $TMAP^{4+}$ and $TMPyP^{4+}$. At a concentration of 1 μM both porphyrins were only slightly effective to inactivate 10^8 CFU/mL after exposure for 30 min to the light emitted by a tungsten–halogen 500 W lamp. When cells were treated with 4 μM porphyrin, $TMPyP^{4+}$ caused only <1 log unit reduction, whereas $TMAP^{4+}$ produced a 3 log units decrease in the cell survival, demonstrating to be largely more efficient against *S. aureus* than $TMPyP^{4+}$. Moreover, the photodynamic killing of microorganisms induced by a series of fullerene derivatives was compared with that mediated by a widely used antimicrobial photosensitizer, toluidine blue O (TBO) [42]. In particular, a monocationic fullerene C_{60} bearing one quaternary pyrrolidinium group (BF4) produced ~3 log of *S. aureus* killing after treatment with 1 μM BF4 and 8 J/cm^2 irradiation with visible light (200 mW/cm^2), while TBO at the same concentration and fluence produced less than 1 log of killing.

In order to obtain information about the efficiency of the dyad **6** in a Gram-negative bacterium, experiments were performed using *E. coli*. Thus, *E. coli* cell suspensions were treated with dyad **6** as described above for *S. aureus*. No toxicity was found in dark even at the higher concentration used (5 μM). After 30 min irradiation with visible light, a decrease of 0.6 log and 1.7 log were obtained for cells incubated with 1 and 5 μM dyad **6**, respectively. It is known that it is easier to inactivate Gram-positive bacteria by PDI than Gram-negative ones [3]. The outer membrane of Gram-negative bacteria forms an effective permeability barrier between the cell and the surrounding medium, tending to restrict the binding and penetration of many photosensitizer structures.

In porphyrin-fullerene C_{60} dyads two processes are competitive. The generation of $O_2(^1\Delta_g)$ from the triplet excited state of the photosensitizer depends on the quantum yield of triplet formation, which goes down if photoinduced electron transfer from the singlet or triplet excited state takes place. This is clear from the solvent effects, specifically there is very little photooxidation of DMA in DMF under conditions where intramolecular electron transfer to generate a charge-separated state occurs. Therefore, the capacity of

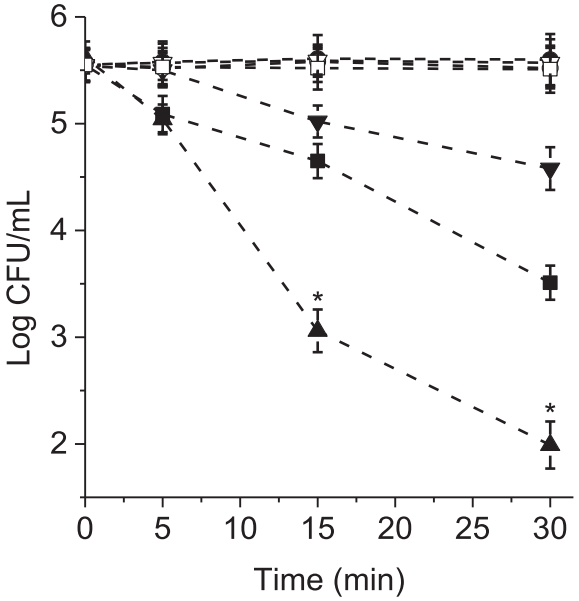

Fig. 7. Survival curves of *S. aureus* cells (~10^6 CFU/mL) incubated with 1 μM DAC_{60}^{+} (▼), TCP^{4+} (■) and **6** (▲) for 30 min at 37 °C in dark and exposed to visible light for different irradiation times. Control cultures: cells treated 1 μM DAC_{60}^{+} (▽), TCP^{4+} (□) and **6** (△) in dark; cells untreated with the photosensitizer and irradiated (●). Values represent mean ± standard deviation of three separate experiments (*$p < 0.05$, compared with DAC_{60}^{+} or TCP^{4+}).

the photosensitizer to generate a charge-separated state on exposure to light could be contributing with its ability to inactivate microorganisms through generation of reactive oxygen species. However, the influence of each mechanism in the photodamage of microorganisms depends on the polarity of the microenvironment where the dyad is localized in the cells.

The combination of hydrophobic and hydrophilic substituents in the photosensitizer results in an amphiphilic molecular structure. This property facilitates membrane penetration and results in better accumulation of the agent in subcellular compartments [4]. In dyad **6**, the presence of cationic groups and the hydrophobic carbon sphere of C_{60} in the same structure produce a considerable increase in the amphiphilic character of the photosensitizer. This effect could help dyads to pass through or accumulate in biomembranes, enhancing the effective photosensitization against *S. aureus*.

4. Conclusions

Porphyrin–fullerene C_{60} dyads with high ability to form photoinduced charge-separated state were evaluated as novel photosensitizers with potential application in the photoinactivation of *S. aureus*. The $O_2(^1\Delta_g)$ productions of these dyads were strongly dependent on the solvent polarity. In more polar solvent, such as DMF, the $O_2(^1\Delta_g)$ generated by dyads was diminished due to stabilization of charge-separated state, while in less polar solvent, such as toluene, the production of $O_2(^1\Delta_g)$ increased. Both dyads interact with toluene/AOT reverse micelles and photosensitized the decomposition of DMA similarly to that observed in toluene. On the other hand, studies *in vitro* of PDI indicated that the photocytotoxic effect on *S. aureus* was higher for cationic **6** than for **5**. These results show that molecular dyads, such as **6**, offer a promising molecular architecture for photosensitizer agents with potential applications in microbial cell photoinactivation.

Acknowledgments

Authors are grateful to Consejo Nacional de Investigaciones Científicas y Técnicas (CONICET) of Argentina (PIP 112-201101-00256), SECYT Universidad Nacional de Río Cuarto (PPI 18/C400) and Agencia Nacional de Promoción Científica y Tecnológica (FONCYT) (PICT-2012-0714) for financial support. M.B.S., M.E.M. and E.N.D. are Scientific Members of CONICET. M.B.B. thanks CONICET for the research fellowship.

References

[1] F.R. DeLeo, M. Otto, B.N. Kreiswirth, H.F. Chambers, Lancet 375 (2010) 1557–1568.
[2] H.F. Chambers, F.R. DeLeo, Nat. Rev. Microbiol. 7 (2009) 629–641.
[3] T. Daia, Y.-Y. Huanga, M.R. Hamblin, Photodiagn. Photodyn. Ther. 6 (2009) 170–188.
[4] E.N. Durantini, Curr. Bioact. Compd. 2 (2006) 127–142.
[5] T.G. St Denis, T. Dai, L. Izikson, C. Astrakas, R.R. Anderson, M.R. Hamblin, G.P. Tegos, Virulence 2 (2011) 509–520.
[6] P.R. Ogilby, Photochem. Photobiol. Sci. 9 (2010) 1543–1560.
[7] M.E. Milanesio, M.G. Alvarez, E.N. Durantini, Curr. Bioact. Compd. 6 (2010) 97–105.
[8] H. Imahori, K. Tamaki, D.M. Guldi, C. Luo, M. Fujitsuka, O. Ito, Y. Sakata, S. Fukuzumi, J. Am. Chem. Soc. 123 (2001) 2607–2617.
[9] P.A. Liddell, G. Kodis, J. Andréasson, L. de la Garza, S. Bandyopadhyay, R.H. Mitchell, T.A. Moore, A.L. Moore, D. Gust, J. Am. Chem. Soc. 126 (2004) 4803–4811.
[10] D.M. Guldi, N. Martin, Functionalized fullerenes: synthesis and functions (chapter 5.13), in: D.L. Andrews, G.D. Scholes, G.P. Wiederrecht (Eds.), Comprehensive Nanoscience and Technology, vol. 5Elsevier B. V., 2011, pp. 379–398.
[11] F. Fungo, L. Otero, C.D. Borsarelli, E.N. Durantini, J.J. Silber, L. Sereno, J. Phys. Chem. B 106 (2002) 4070–4078.
[12] M.E. Milanesio, M.G. Alvarez, V. Rivarola, J.J. Silber, E.N. Durantini, Photochem. Photobiol. 81 (2005) 891–897.
[13] M.G. Alvarez, C. Prucca, M.E. Milanesio, E.N. Durantini, V. Rivarola, Int. J. Biochem. Cell. Biol. 38 (2006) 2092–2101.
[14] S. Issa, N. Walchshofer, I. Kassab, H. Termoss, S. Chamat, A. Geahchan, Z. Bouaziz, Eur. J. Med. Chem. 45 (2010) 2567–2577.
[15] T.H. Xu, R. Lu, X.P. Qiu, X.L. Liu, P.C. Xue, C.H. Tan, C.Y. Bao, Y.Y. Zhao, Eur. J. Org. Chem. 2006 (2006) 4014–4020.
[16] J. Durantini, L. Otero, M. Funes, E.N. Durantini, F. Fungo, M. Gervaldo, Electrochim. Acta 56 (2011) 4126–4134.
[17] M.E. Milanesio, M.G. Alvarez, J.J. Silber, V. Rivarola, E.N. Durantini, Photochem. Photobiol. Sci. 2 (2003) 926–933.
[18] M.E. Milanesio, E.N. Durantini, Synth. Commun. 36 (2006) 2135–2144.
[19] F. Fungo, M.E. Milanesio, E.N. Durantini, L. Otero, T. Dittrich, J. Mater. Chem. 17 (2007) 2107–2112.
[20] M.B. Spesia, M.E. Milanesio, E.N. Durantini, Eur. J. Med. Chem. 43 (2008) 853–861.
[21] D.D. Ferreyra, M.B. Spesia, M.E. Milanesio, E.N. Durantini, J. Photochem. Photobiol. A – Chem. 282 (2014) 16–24.
[22] M.E. Milanesio, M.G. Alvarez, E.I. Yslas, C.D. Borsarelli, J.J. Silber, V. Rivarola, E.N. Durantini, Photochem. Photobiol. 74 (2001) 14–21.
[23] M. Novaira, M.P. Cormick, E.N. Durantini, J. Photochem. Photobiol. A – Chem. 246 (2012) 67–74.
[24] J.J. Silber, A. Biasutti, E. Abuin, E. Lissi, Adv. Colloid Interface Sci. 82 (1999) 189–252.
[25] E.N. Durantini, J.J. Silber, Synth. Commun. 29 (1999) 3353–3368.
[26] E.N. Durantini, J. Porphyr. Phthalocyan. 4 (2000) 233–242.
[27] T. Hashimoto, Y.-K. Choe, H. Nakano, K. Hirao, J. Phys. Chem. A 103 (1999) 1894–1904.
[28] R.V. Maximiano, E. Piovesan, S.C. Zílio, A.E.H. Machado, R. de Paula, J.A.S. Cavaleiro, I.E. Borissevitch, A.S. Ito, P.J. Gonçalves, N.M. Barbosa Neto, J. Photochem. Photobiol. A – Chem. 214 (2010) 115–120.
[29] J.S. Baskin, H.-Z. Yu, A.H. Zewail, J. Phys. Chem. A 106 (2002) 9837–9844.
[30] S.J. Mora, M.P. Cormick, M.E. Milanesio, E.N. Durantini, Dyes Pigm. 87 (2010) 234–240.
[31] D.I. Schuster, K. Li, D.M. Guldi, A. Palkar, L. Echegoyen, C. Stanisky, R.J. Cross, M. Niemi, N.V. Tkachenko, H. Lemmetyinen, J. Am. Chem. Soc. 129 (2007) 15973–15982.
[32] D.A. Caminos, M.B. Spesia, E.N. Durantini, Photochem. Photobiol. Sci. 5 (2006) 56–65.
[33] D. Rehm, A. Weller, Isr. J. Chem. 7 (1970) 259–271.
[34] P.K. Poddutoori, A.S.D. Sandanayaka, N. Zarrabi, T. Hasobe, O. Ito, A. van der Est, J. Phys. Chem. A 115 (2011) 709–717.
[35] A. Gomes, E. Fernandes, J.L.F.C. Lima, J. Biochem. Biophys. Methods 65 (2005) 45–80.
[36] R.W. Redmond, J.N. Gamlin, Photochem. Photobiol. 70 (1999) 391–475.
[37] I. Scalise, E.N. Durantini, J. Photochem. Photobiol. A – Chem. 162 (2004) 105–113.
[38] A.L. Ochoa, T.C. Tempesti, M.B. Spesia, M.E. Milanesio, E.N. Durantini, Eur. J. Med. Chem. 50 (2012) 280–287.
[39] C.D. Borsarelli, E.N. Durantini, N.A. García, J. Chem. Soc. Perkin Trans. 2 (1996) 2009–2013.
[40] E. Reddi, M. Ceccon, G. Valduga, G. Jori, J.C. Bommer, F. Elisei, L. Latterini, U. Mazzucato, Photochem. Photobiol. 75 (2002) 462–470.
[41] S. Banfi, E. Caruso, L. Buccafurni, V. Battini, S. Zazzaron, P. Barbieri, V. Orlandi, J. Photochem. Photobiol. B – Biol. 85 (2006) 28–38.
[42] G.P. Tegos, T.N. Demidova, D. Arcila-Lopez, H. Lee, T. Wharton, H. Gali, M.R. Hamblin, Chem. Biol. 12 (2005) 1127–1135.